Magnetic Reconnection and Particle Acceleration during Kinetic Magneto-Rotational Instability in an Accretion Disk

M. Hoshino, K. Shirakawa and K. Hirabayashi
University of Tokyo

Plasma processes in Accretion Disk

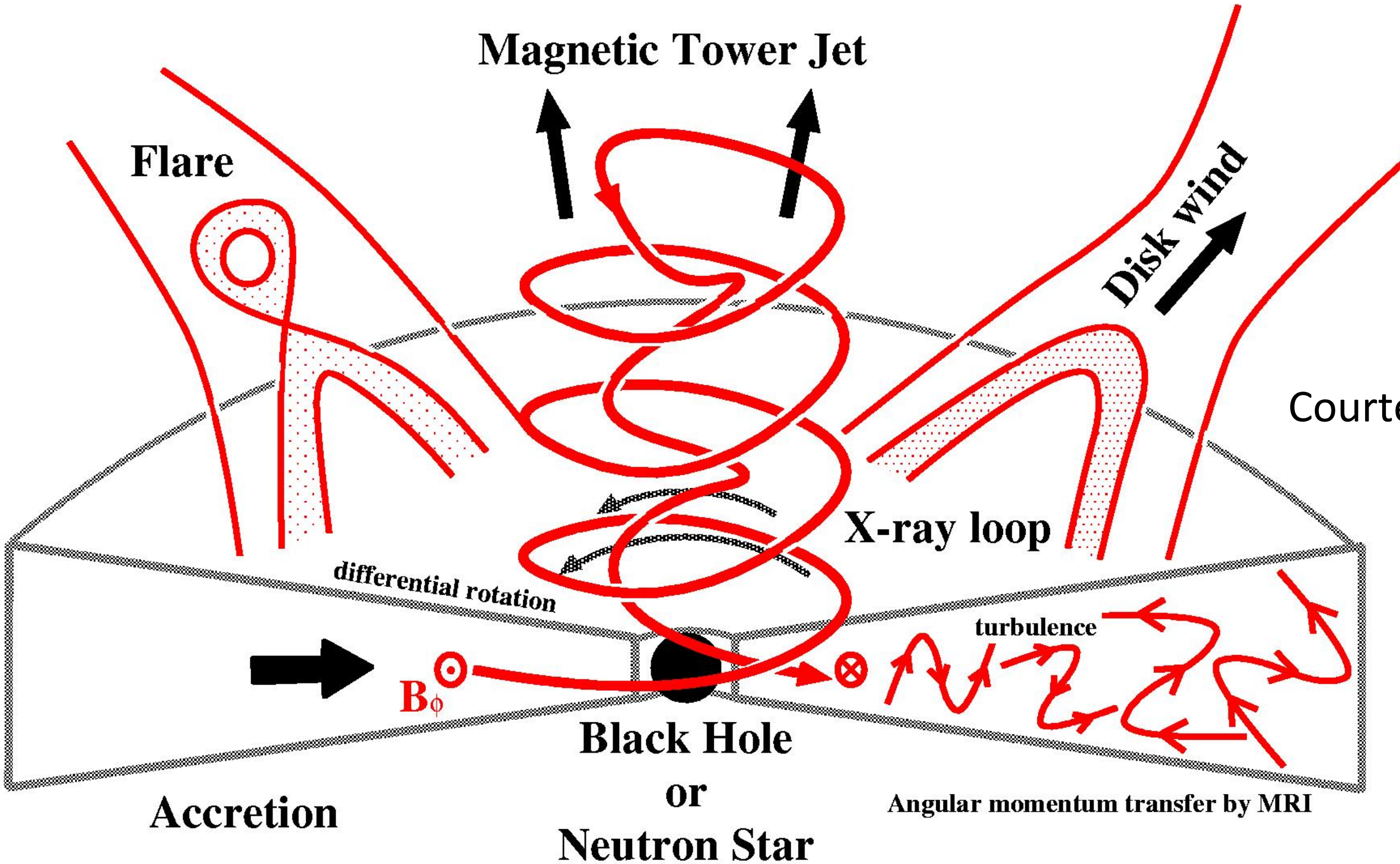

Courtesy of Kato

Magneto-Rotational Instability (MRI)

Velikov 1958, Chandrasekhar 1961, Balbus & Hawly 1991

Magneto-Rotational Instability (MRI)

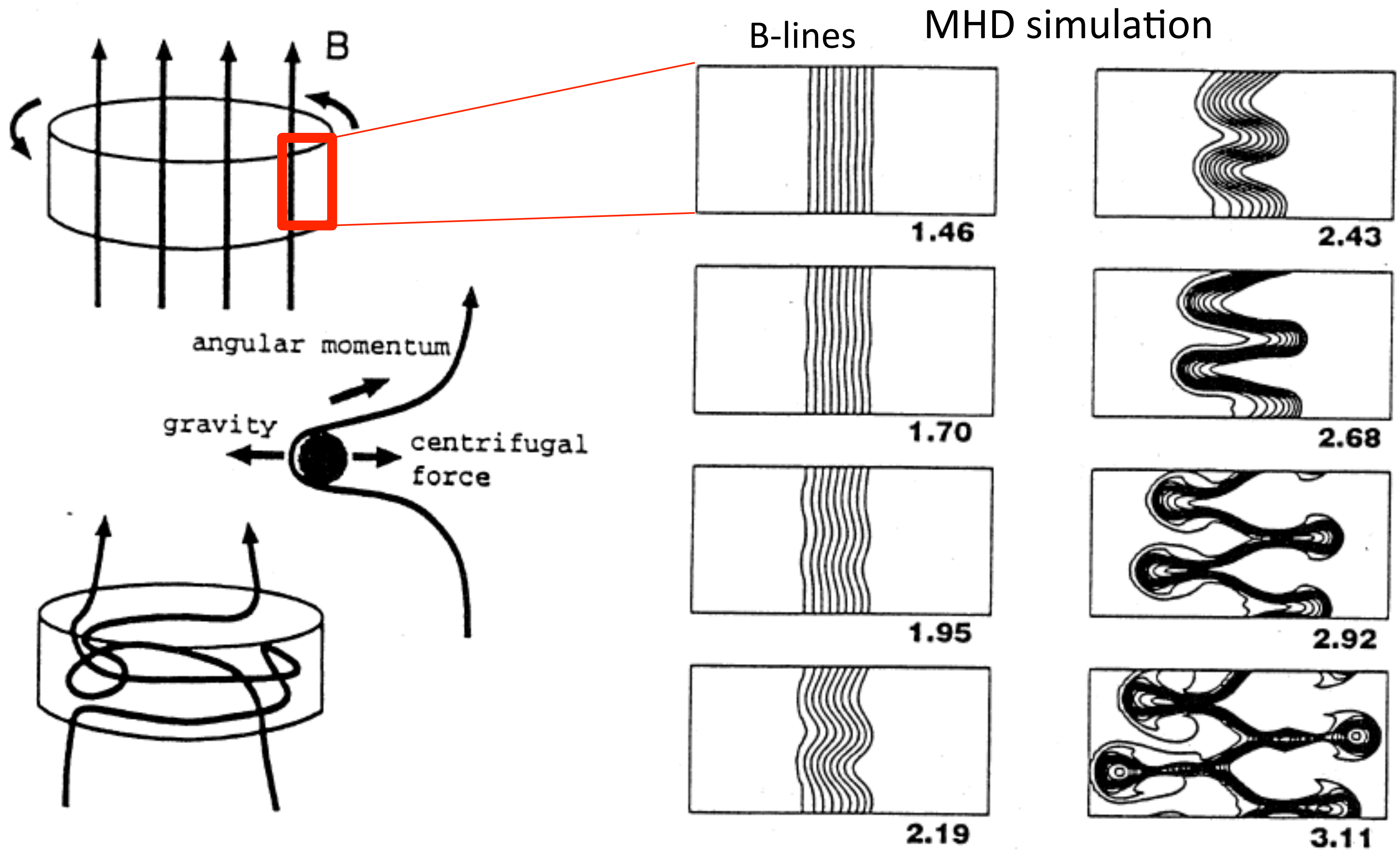

weak magnetic field (β>>1) → β = 1-10
dynamo process

Balbus and Hawley, 1998

Collisionless Accretion Disk?

- *Massive black hole (Sgr A*)*
- Radiatively Inefficient Accretion Flow (RIAF)
- Accretion rate much smaller than the Bondi rate of $10^{-5} M_*/yr$ → net accretion rate $10^{-8} M_*/yr$
- thermal and nonthermal electrons (X-ray flare by observed Chandra & XMM-Newton), power law index $p \sim 1.3 < 2$

→Kinetic Magneto-Rotational Instability (MRI) and particle acceleration

“Collisionless” MRI

MHD + Landau Fluid Approx.

$$\frac{\partial \rho}{\partial t} + \nabla \cdot (\rho \boldsymbol{V}) = 0,$$

$$\rho \frac{\partial \boldsymbol{V}}{\partial t} + \rho(\boldsymbol{V} \cdot \nabla)\boldsymbol{V} = \frac{(\nabla \times \boldsymbol{B}) \times \boldsymbol{B}}{4\pi} - \nabla \cdot \boldsymbol{P} + \boldsymbol{F_g},$$

$$\frac{\partial \boldsymbol{B}}{\partial t} = \nabla \times (\boldsymbol{V} \times \boldsymbol{B}),$$

$$\boldsymbol{P} = p_\perp \boldsymbol{I} + (p_\parallel - p_\perp)\hat{\boldsymbol{b}}\hat{\boldsymbol{b}} = p_\perp \boldsymbol{I} + \boldsymbol{\Pi},$$

$$\rho B \frac{D}{Dt}\left(\frac{p_\perp}{\rho B}\right) = -\nabla \cdot \boldsymbol{q}_\perp - q_\perp \nabla \cdot \hat{\boldsymbol{b}},$$

$$\frac{\rho^3}{B^2}\frac{D}{Dt}\left(\frac{p_\parallel B^2}{\rho^3}\right) = -\nabla \cdot \boldsymbol{q}_\parallel + 2 q_\perp \nabla \cdot \hat{\boldsymbol{b}},$$

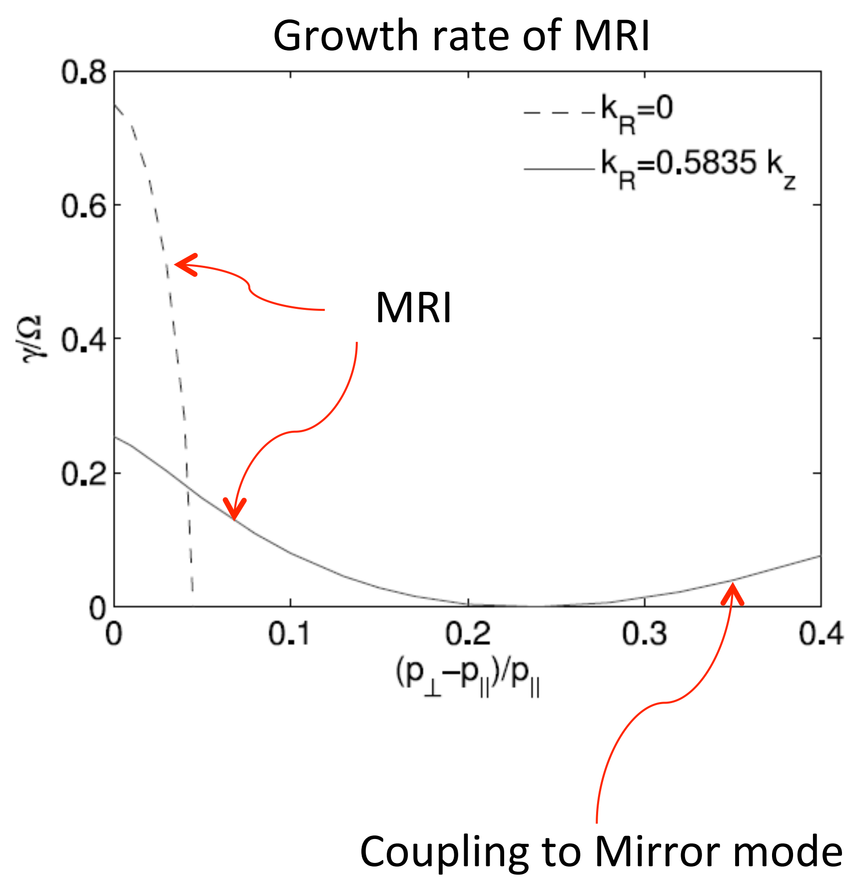

(Quataert+, ApJ, 2002; Sharma+, ApJ, 2006)

MRI and Reconnection in PIC simulation

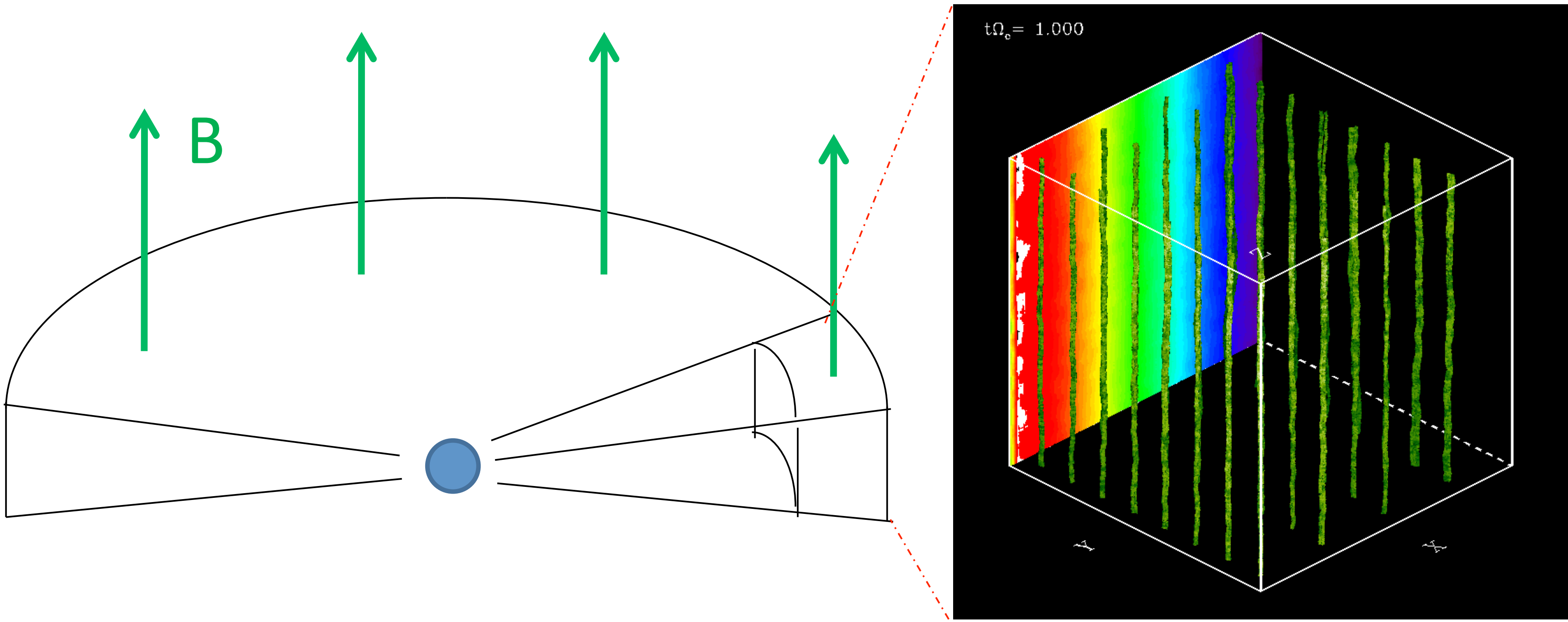

green: magnetic field lines
color contour: angular velocity

β=100, Kepler rotation Ω
256x256x256 grids 40 particles/cell,
periodic shearing box,
electron-positron plasma

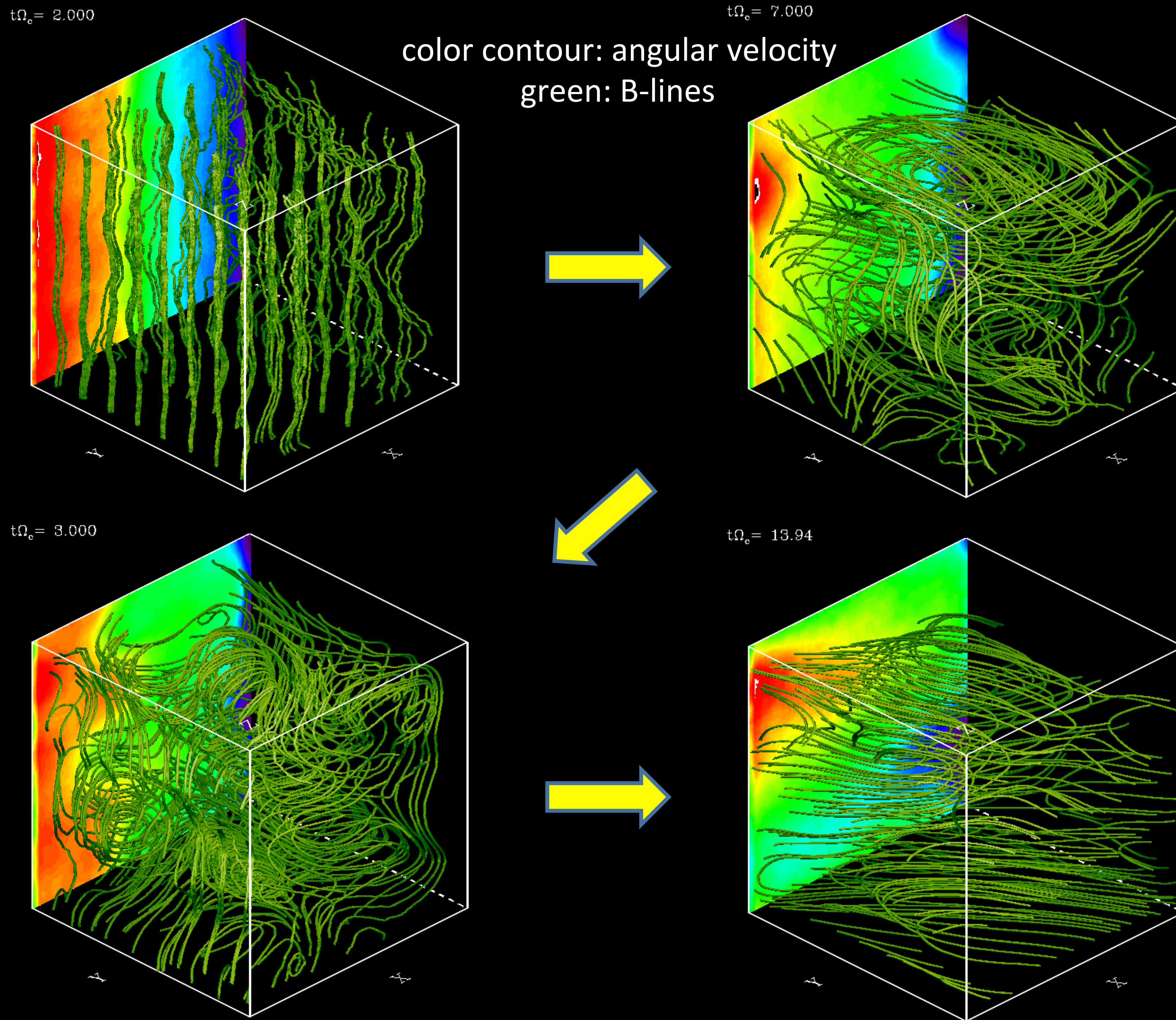
color contour: angular velocity
green: B-lines
tΩc= 2.000
tΩc= 7.000
tΩc= 3.000
tΩc= 13.94
Y
X

2D-PIC simulation

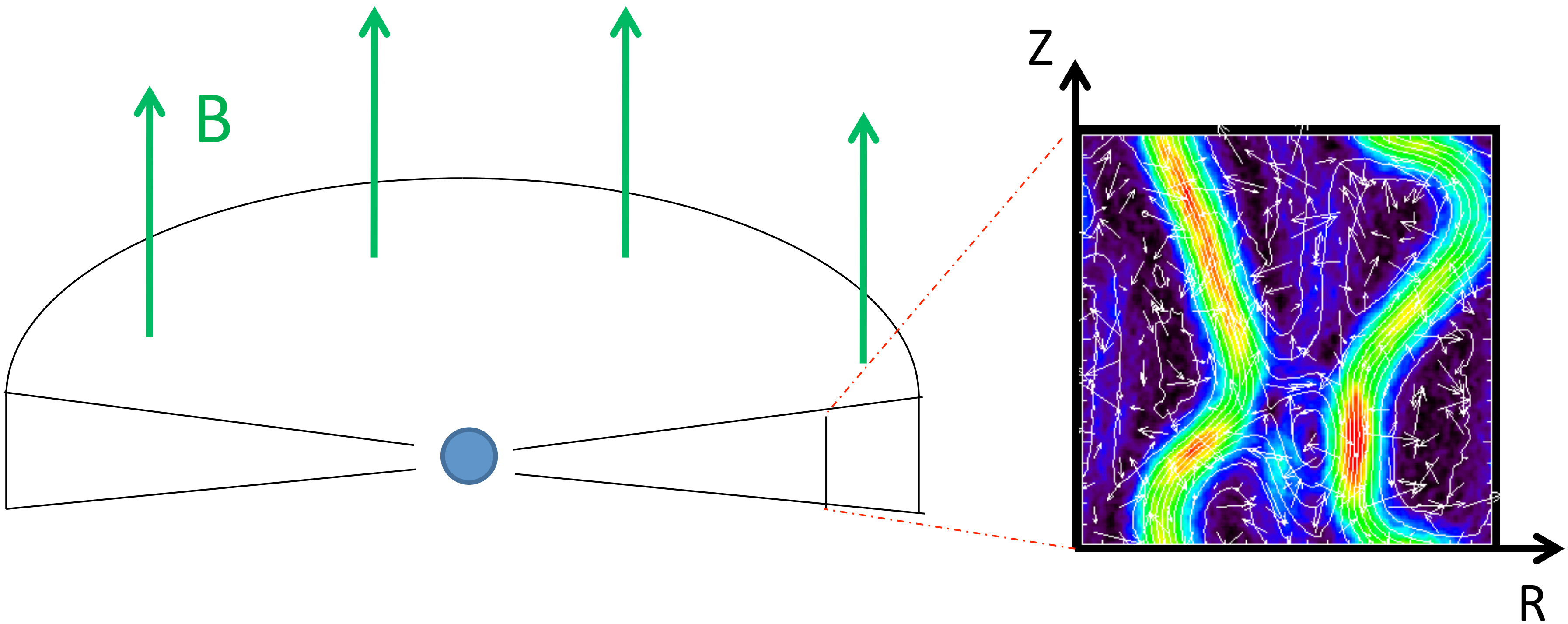

Kepler rotation Ω, $\Omega / \Omega_c = 0.1$,
gyro-radius $V_i / \Omega_c = 1.7\times10^2$ at t=0
β=20000, 200x200 grids 8000 particles/cell,
periodic box in meridian plane, electron-positron plasma

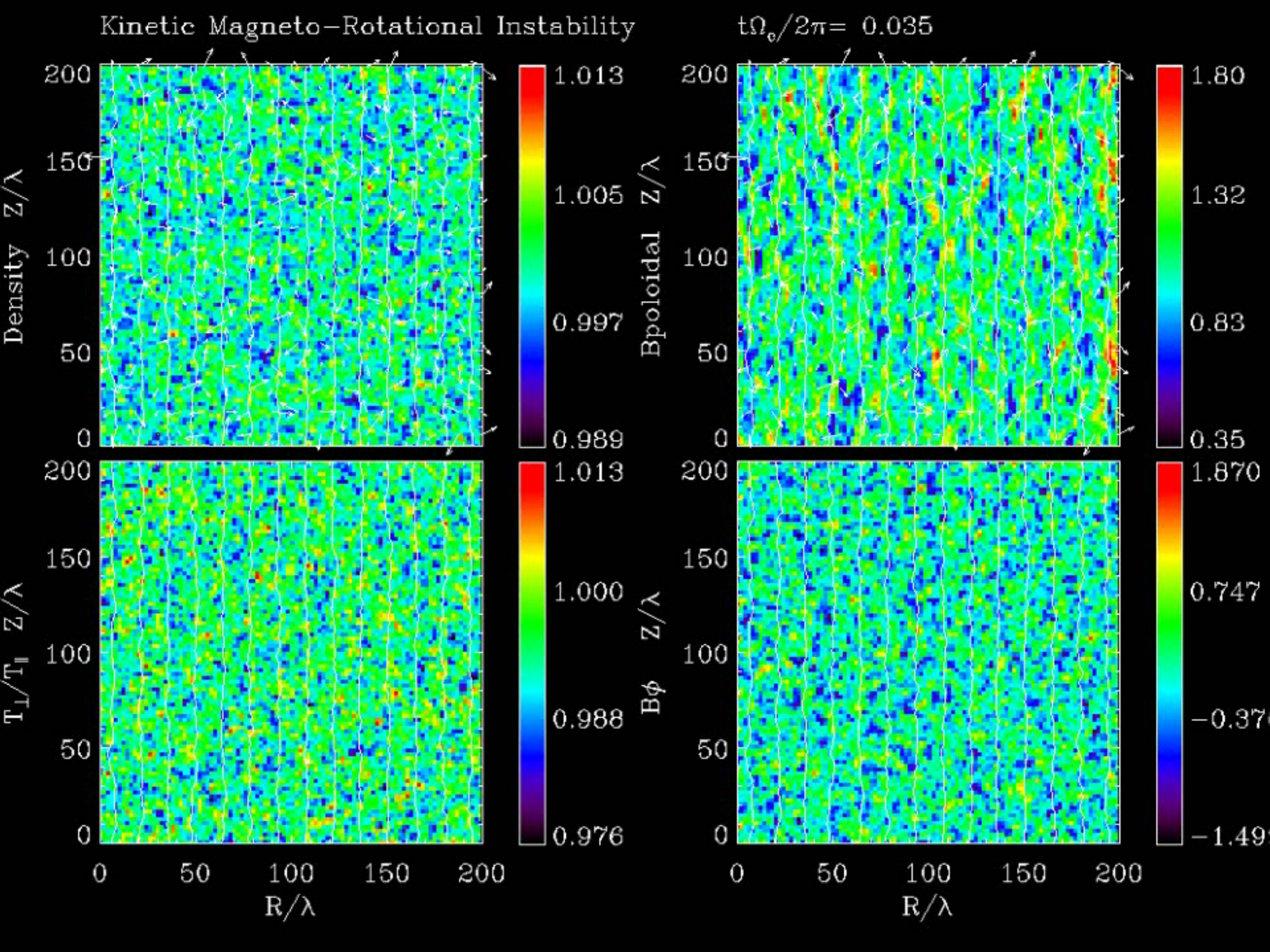

Kinetic Magneto-Rotational Instability
$t\Omega_c/2\pi = 0.035$
Density Z/λ
1.013
1.005
0.997
0.989
Bpoloidal Z/λ
1.80
1.32
0.83
0.35
$T_\perp/T_\parallel$ Z/λ
1.013
1.000
0.988
0.976
Bφ Z/λ
1.870
0.747
R/λ
R/λ
0
50
100
150
200

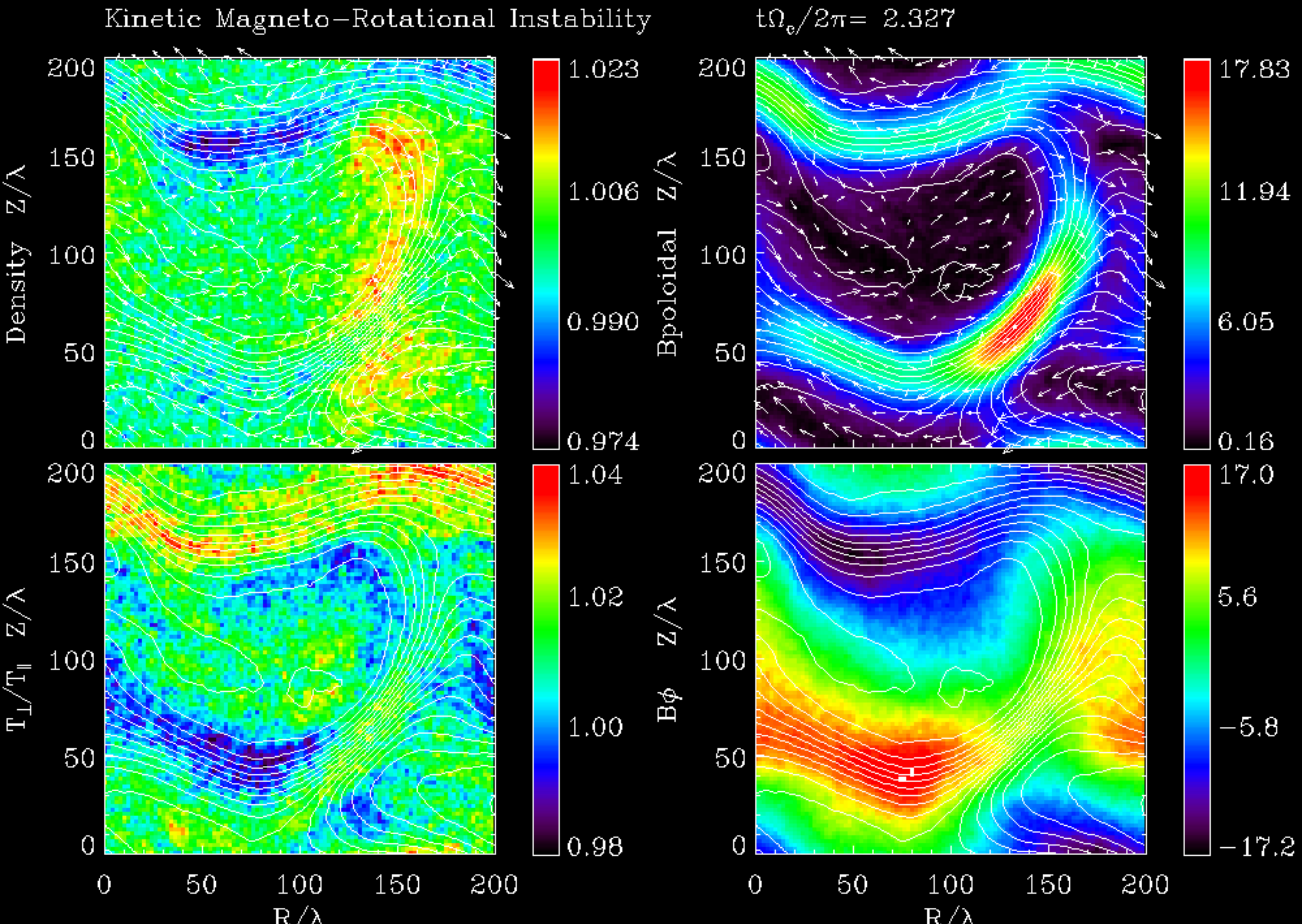

Kinetic Magneto-Rotational Instability
$t\Omega_c/2\pi$= 2.327
Density Z/λ
Bpoloidal Z/λ
$T_\perp/T_\parallel$ Z/λ
Bφ Z/λ
R/λ
R/λ
1.023
1.006
0.990
0.974
17.83
11.94
6.05
0.16
1.04
1.02
1.00
0.98
17.0
5.6
−5.8
−17.2

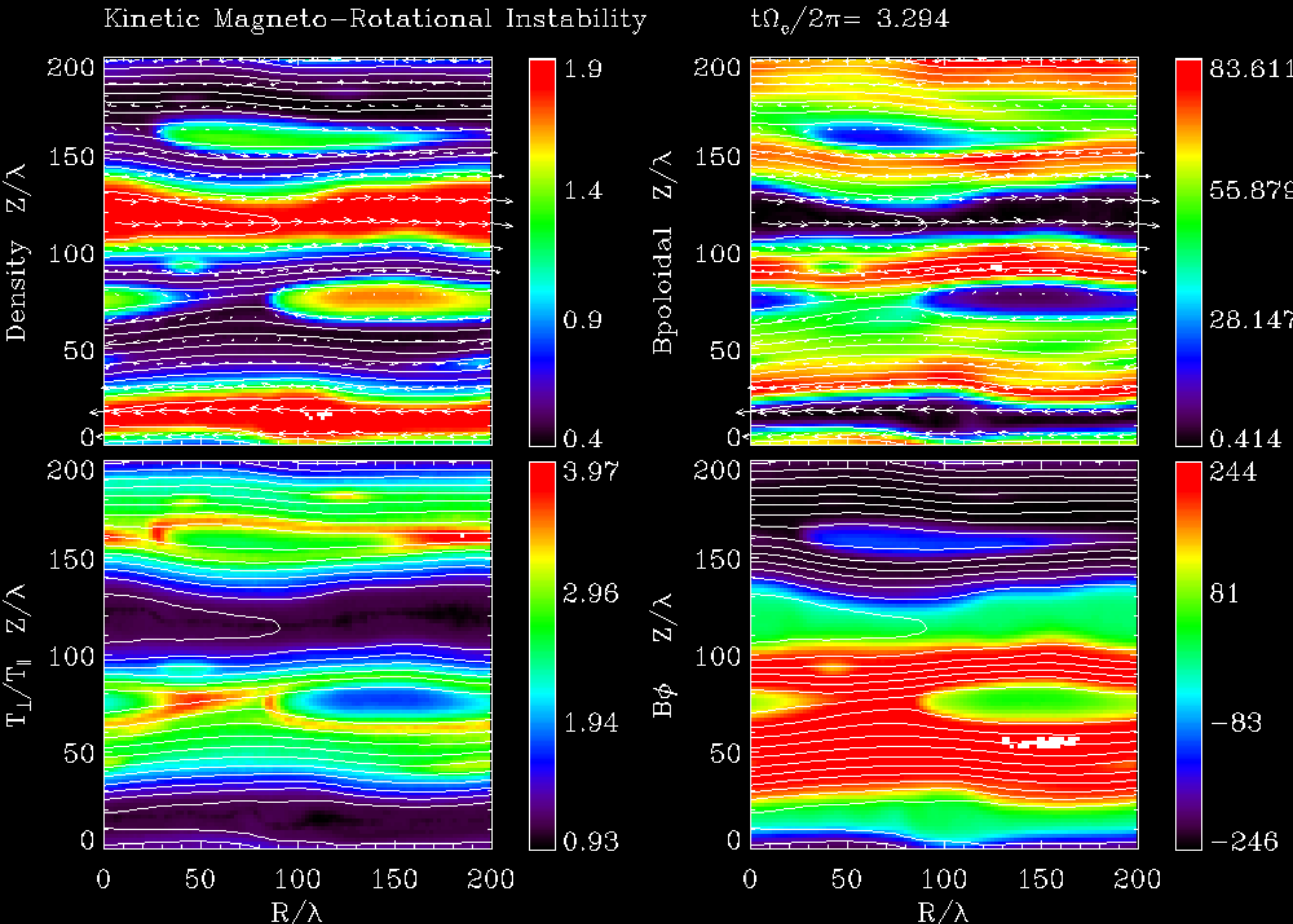

Kinetic Magneto-Rotational Instability
$t\Omega_c/2\pi$= 3.294
Density Z/λ
1.9
1.4
0.9
0.4
Bpoloidal Z/λ
83.611
55.879
28.147
0.414
$T_\perp/T_\parallel$ Z/λ
3.97
2.96
1.94
0.93
Bφ Z/λ
244
81
−83
−246
0
50
100
150
200
R/λ

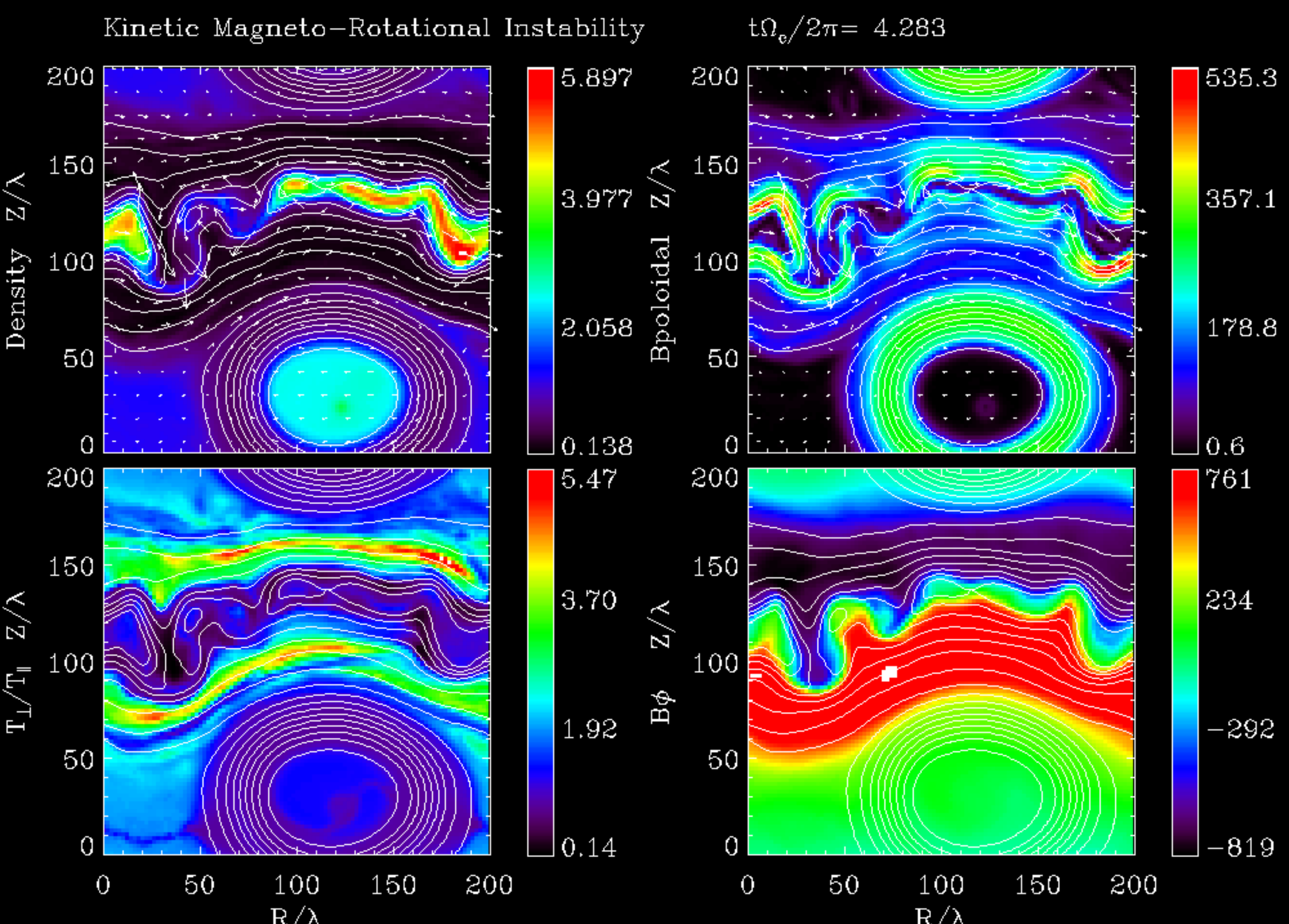
Kinetic Magneto-Rotational Instability
tΩ_c/2π= 4.283
Density Z/λ
5.897
3.977
2.058
0.138
Bpoloidal Z/λ
535.3
357.1
178.8
0.6
T⊥/T∥ Z/λ
5.47
3.70
1.92
0.14
Bφ Z/λ
761
234
−292
−819
R/λ
R/λ

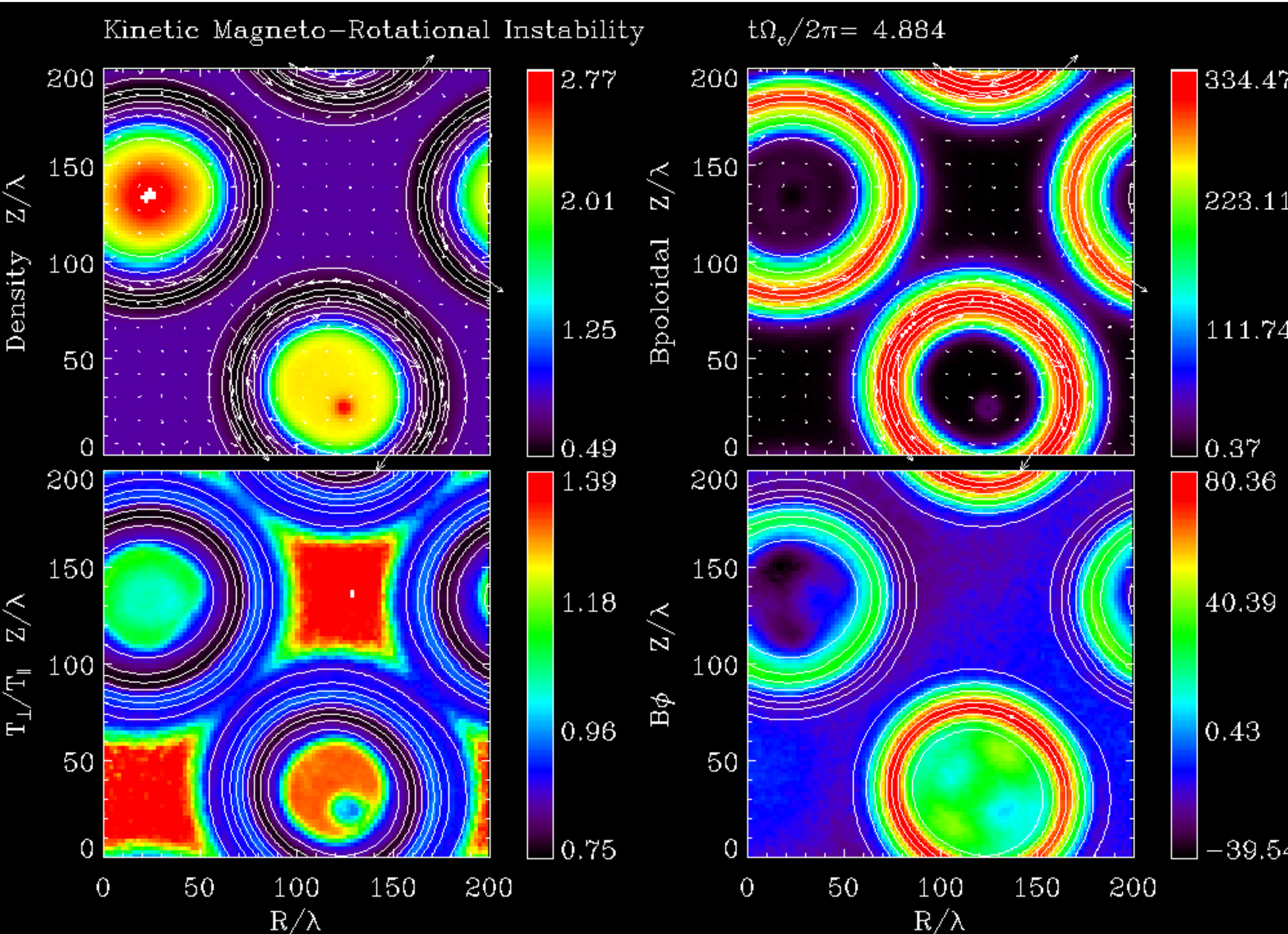

Kinetic Magneto-Rotational Instability
tΩc/2π= 4.884
Density Z/λ
2.77
2.01
1.25
0.49
Bpoloidal Z/λ
334.47
223.11
111.74
0.37
T⊥/T∥ Z/λ
1.39
1.18
0.96
0.75
Bφ Z/λ
80.36
40.39
0.43
−39.54
R/λ
R/λ
0
50
100
150
200

Onset of Reconnection

Before Reconnection | After onset of Reconnection

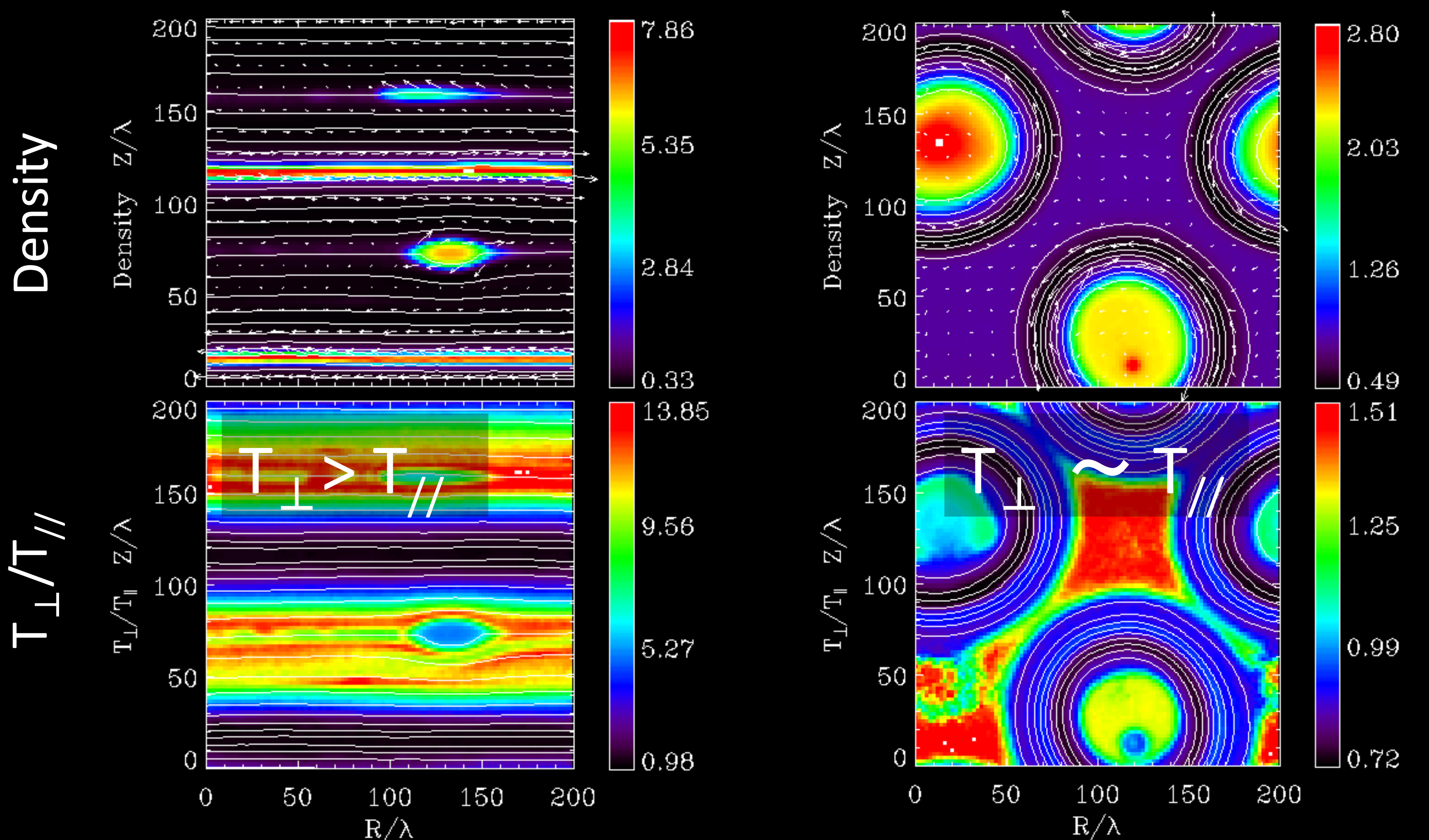

Growth rate of tearing mode is enhanced for $T_\perp > T_{//}$

Laval and Pellat (1968), Chen and Palmadesso (1984)

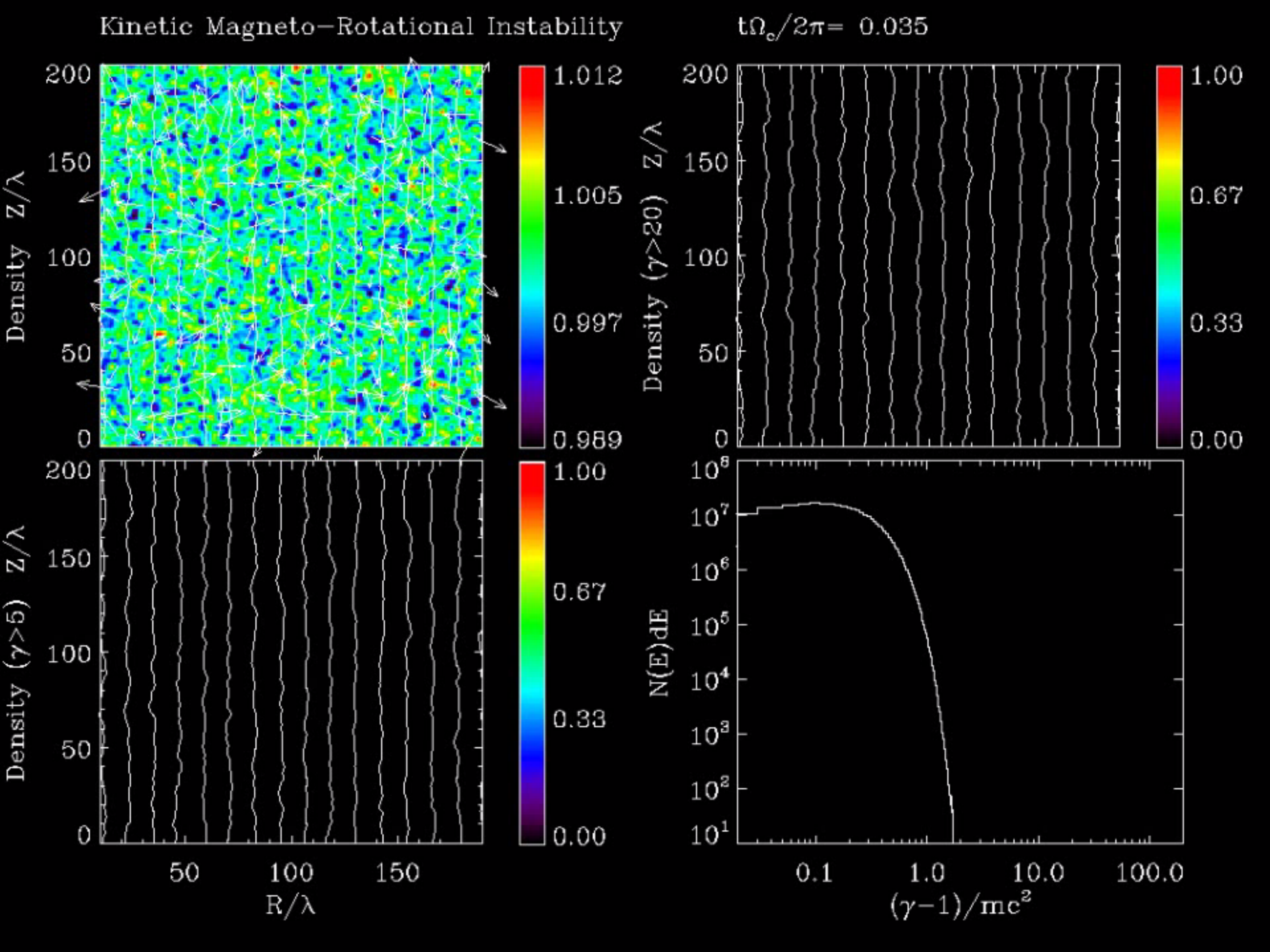

Kinetic Magneto–Rotational Instability
tΩ_c/2π= 0.035
Density Z/λ
Density (γ>20) Z/λ
Density (γ>5) Z/λ
N(E)dE
R/λ
(γ−1)/mc²
1.012
1.005
0.997
0.989
1.00
0.67
0.33
0.00
0.1
1.0
10.0
100.0

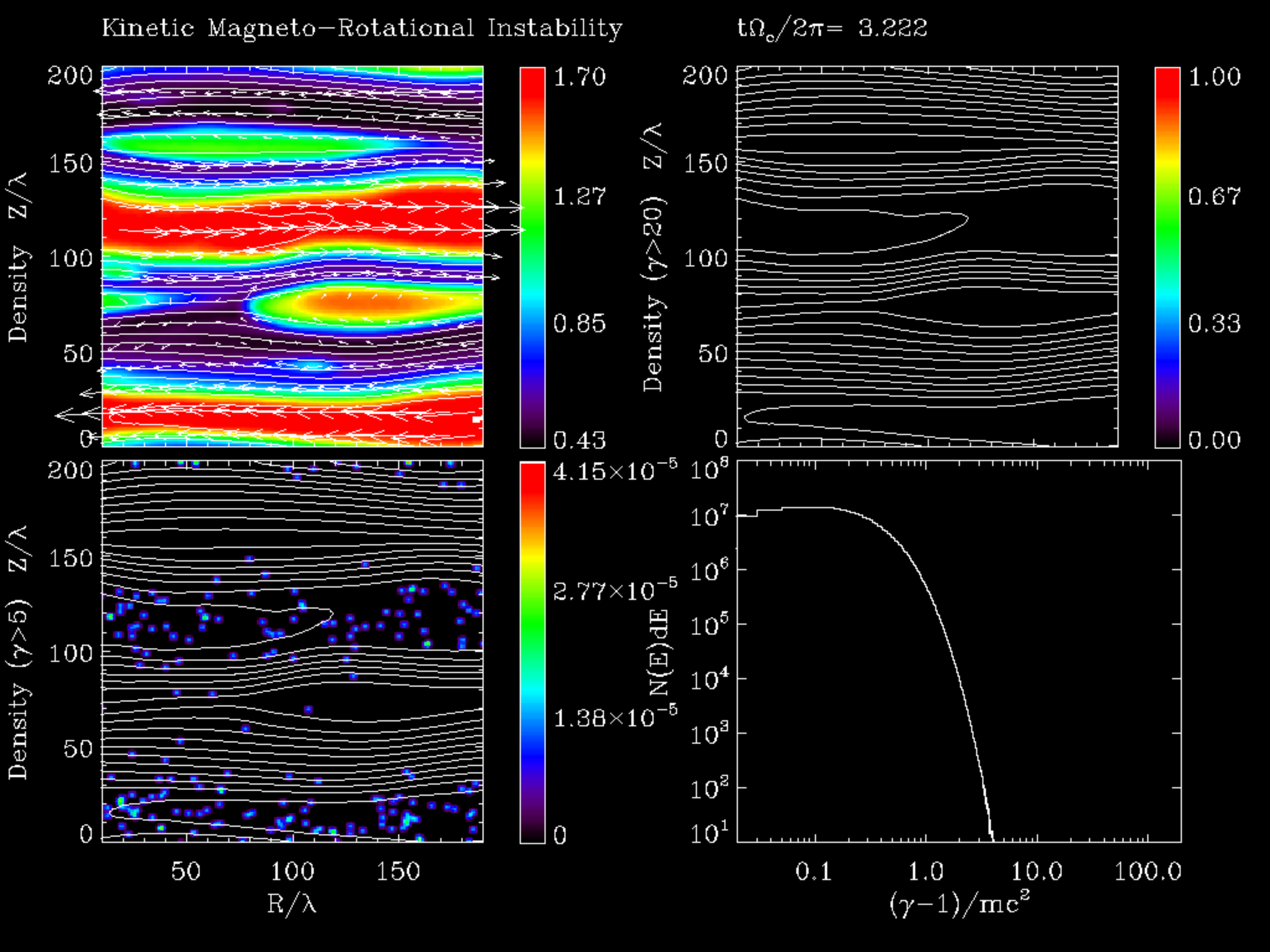

Kinetic Magneto-Rotational Instability
tΩ_c/2π= 3.222
Density Z/λ
Density (γ>20) Z/λ
Density (γ>5) Z/λ
R/λ
N(E)dE
(γ-1)/mc²
1.70
1.27
0.85
0.43
1.00
0.67
0.33
0.00
4.15×10⁻⁵
2.77×10⁻⁵
1.38×10⁻⁵
0

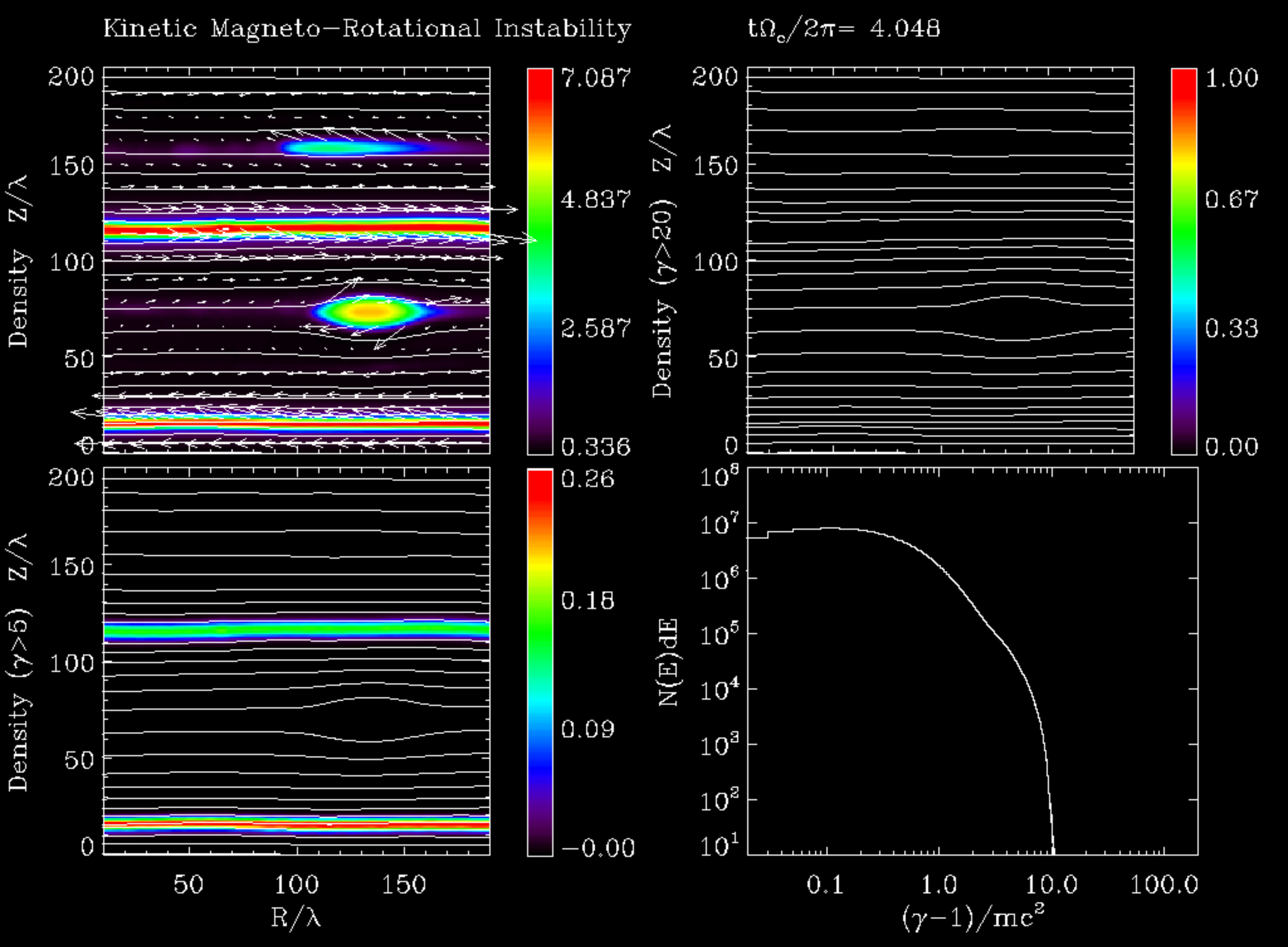
Kinetic Magneto-Rotational Instability
tΩc/2π= 4.048
Density Z/λ
7.087
4.837
2.587
0.336
Density (γ>20) Z/λ
1.00
0.67
0.33
0.00
Density (γ>5) Z/λ
0.26
0.18
0.09
−0.00
R/λ
N(E)dE
(γ−1)/mc²
200
150
100
50
0
0.1
1.0
10.0
100.0

thermal plasma is confined inside magnetic islands

high energetic particles (γ>20) are located outside magnetic islands

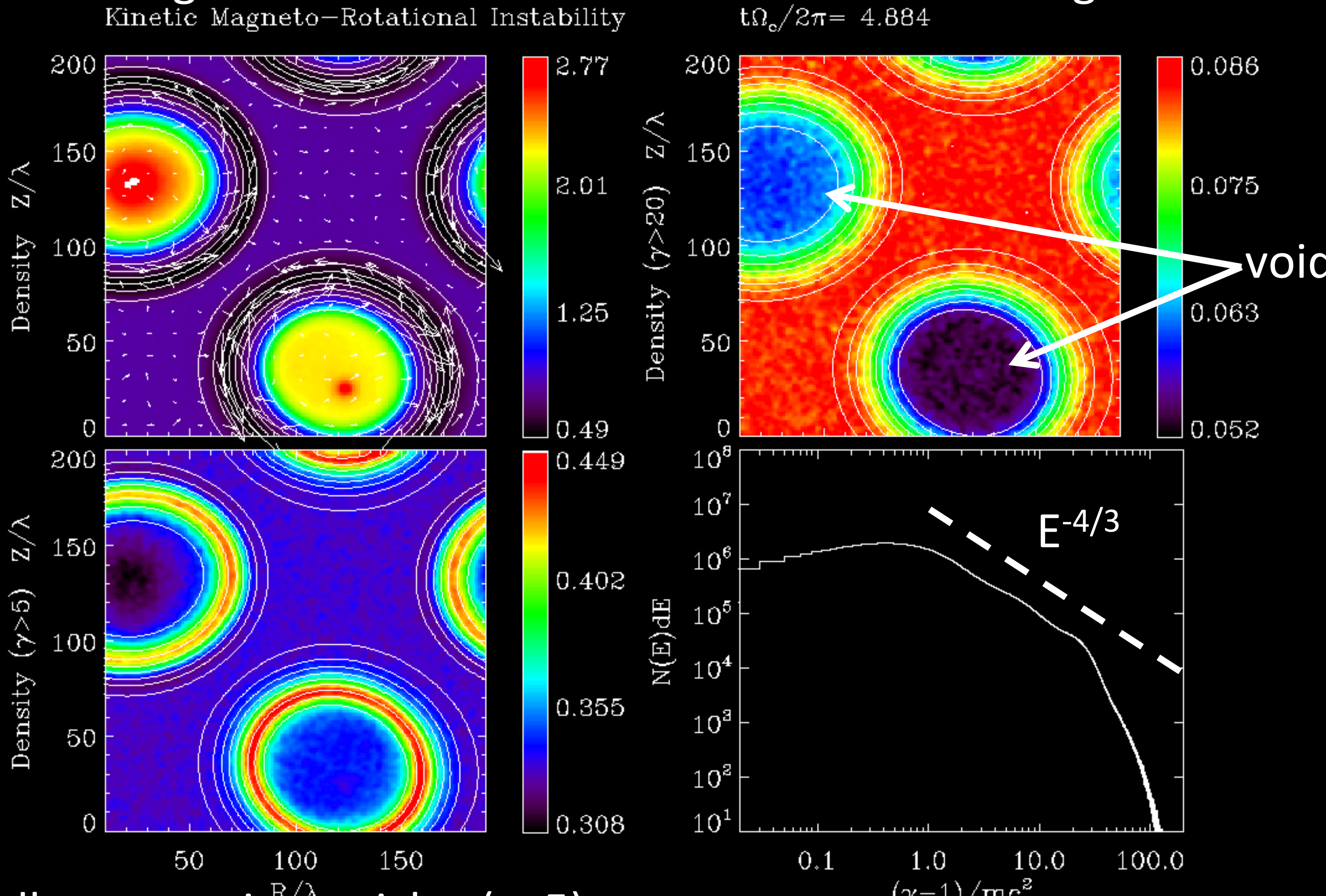

middle energetic particles (γ>5) are located at outer edge of islands

Fermi acceleration in magnetic islands

2^{nd} order Acceleration

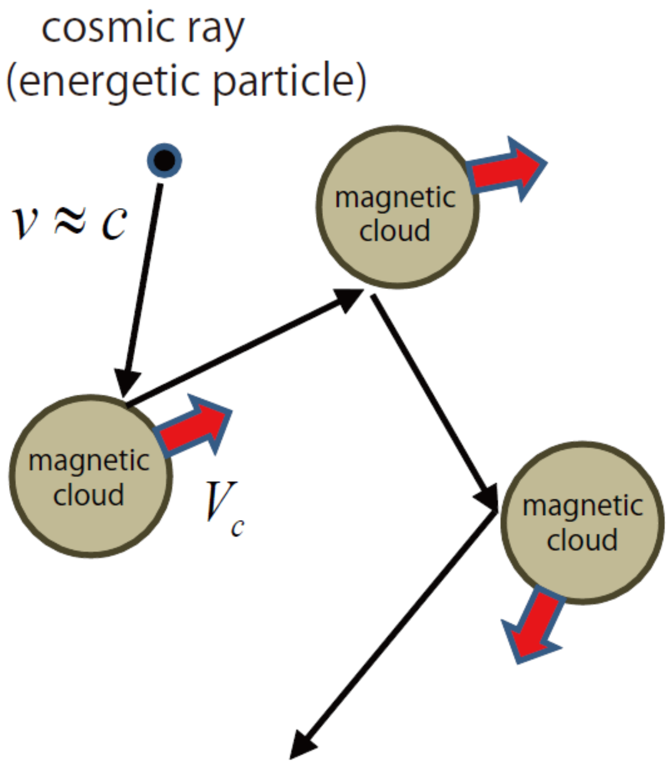

$$\frac{\Delta\varepsilon}{\varepsilon} \approx \left(\frac{V_c}{c}\right)^2$$

Fermi, Phys. Rev. (1949)

1^{st} order Acceleration

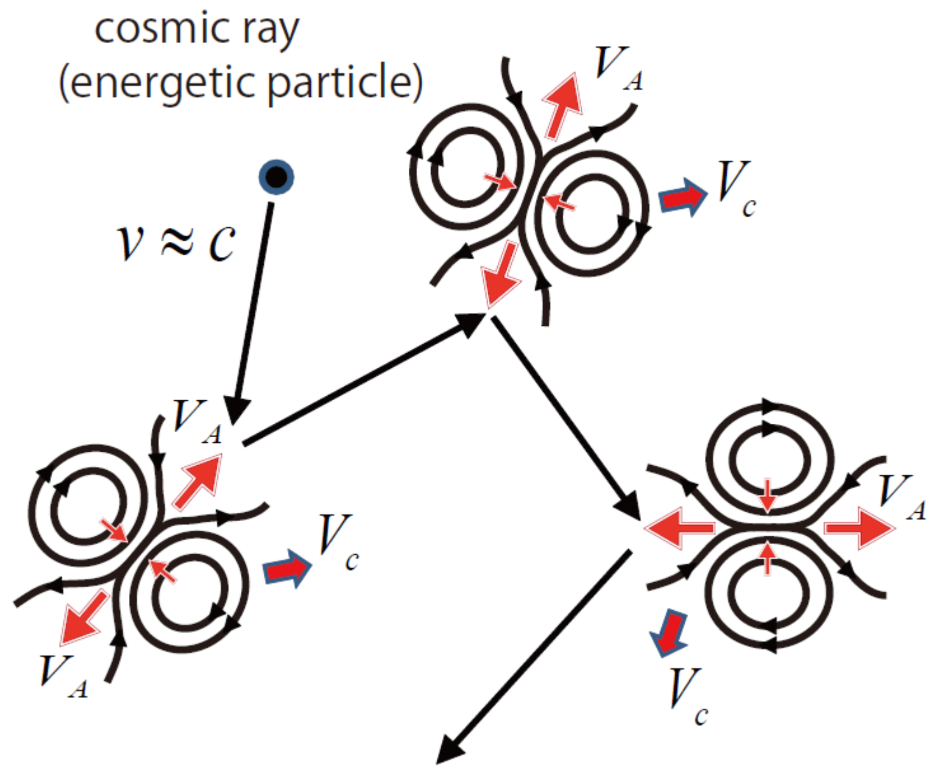

$$\frac{\Delta\varepsilon}{\varepsilon} \approx \left(\frac{V_A}{c}\right)$$

MH, PRL (2012)

Summary

- Collisionless Magneto-Rotational Instability
  - $T_{\perp} > T_{//}$ during MRI evolution
  - Enhanced Reconnection due to $T_{\perp} > T_{//}$
  - X-type acceleration in a stretched magnetic field due to MRI channel flow
  - Hard energy spectrum with $N(E) \propto E^{-1.3}$ (in 2d PIC simulation)
  - More particle acceleration by multiple magnetic island reconnection in a large scale system